J|A|C|S
ARTICLES
Published on Web 11/24/2004

Conformational Change of H^+-ATPase β Monomer Revealed on Segmental Isotope Labeling NMR Spectroscopy

Hiromasa Yagi,† Takuya Tsujimoto,† Toshio Yamazaki,‡ Masasuke Yoshida,§ and Hideo Akutsu*,†

Contribution from the Institute for Protein Research, Osaka University, 3-2 Yamadaoka, Suita 565-0871, Japan, Genome Sciences Center, RIKEN Yokohama Institute, 1-7-22 Suehirocho, Tsurumi-ku, Yokohama 230-0045, Japan, and Chemical Resources Laboratory, Tokyo Institute of Technology, Nagatsuta 4259, Yokohama 226-8503, Japan

Received August 5, 2004; E-mail: akutsu@protein.osaka-u.ac.jp

Abstract: F_1-ATPase has been shown to be a stepwise molecular motor. Its rotation mechanism has been explained by the interaction of the γ axis with the open and closed forms of the β subunit. Although NMR should be a powerful method for elucidating its mechanism, its molecular size (473 amino acid residues, 52 kDa) is a major obstacle. We have applied segmental labeling based on intein ligation to the β subunit, and succeeded in assigning 89% of the NH (402/451), 89% of the C_α (417/473), 83% of the C_β (357/431), and 90% of the CO (425/473) signals of the β subunit monomer. The secondary structures predicted from the chemical shifts of the main chain atoms and the relative orientations determined from residual dipolar couplings indicated that the subunit β monomer takes on the open form in the absence of nucleotide. Furthermore, the chemical shift perturbation and the residual-dipolar-coupling changes induced by nucleotide binding show that conformational change from the open to the closed form takes place on nucleotide binding. The intrinsic conformational change of the β subunit monomer induced by nucleotide binding must be one of the essential driving forces for the rotation of F_1-ATPase.

Introduction

F_OF_1-ATP synthase is a multisubunit enzyme that catalyzes ATP synthesis in oxidative phosphorylation and photophosphorylation using the electrochemical potential of a proton gradient.[1−4] This enzyme consists of two components, F_O and F_1. The simplest F_1 (F_1-ATPase) comprises five kinds of subunits with a stoichiometry of $\alpha_3\beta_3\gamma\delta\epsilon$.[5,6] The catalytic site is located in the β subunit at the α-β interface.[1,7,8] In the crystal structure of F_1 from bovine heart mitochondria (MF_1), the three catalytic sites are not equivalent.[8] The β subunit in F_1 takes on the closed form in the presence of a bound nucleotide, while it takes on the open form in its absence. Recently, a half-closed conformation of the β subunit was reported for MF_1, which was assumed to be a transient conformation during the release of ($ADP+P_i$).[9] F_1-ATPase has been shown to be a stepwise molecular motor.[10,11] Its rotation mechanism is explained by the interaction of the γ subunit in the center with the open and closed forms of the β subunit. We have proposed, on the basis of ^1H NMR experiments, that the β subunit monomer has an intrinsic ability to change the conformation from the open to the closed form on the binding of a nucleotide, which could be one of the essential driving forces for the F_1 rotation.[12,13] Since the β subunit consists of 473 amino acid residues (52 kDa),[14] its molecular mass was much larger than the molecular limit for NMR analysis. Thus, the information obtained so far by ^1H NMR has been limited.

The size limit is caused by the signal broadening due to rapid transverse relaxation in a slowly tumbling molecule and by the signal overlapping due to the huge number of resonating nuclear spins in a protein. The former has been improved by means of deuteration of the protein[15,16] and innovative pulse techniques. Development of TROSY spectroscopy has contributed to a revolutionary improvement of the resolution of $^1H-^{15}N$ and $^1H-^{13}C$(aromatic) correlation spectra.[17] The combination of deuteration and TROSY raised the molecular mass limit to more than 50 kDa. For example, the assignment of a dimeric construct

† Institute for Protein Research, Osaka University.
‡ Genome Sciences Center, RIKEN Yokohama Institute.
§ Chemical Resources Laboratory, Tokyo Institute of Technology.

(1) Boyer, P. D. *Annu. Rev. Biochem.* **1997**, *66*, 717−749.
(2) Stock, D.; Gibbons, C.; Arechaga, I.; Leslie, A. G.; Walker, J. E. *Curr. Opin. Struct. Biol.* **2000**, *10*, 672−679.
(3) Yoshida, M.; Muneyuki, E.; Hisabori, T. *Nat. Rev. Mol. Cell Biol.* **2001**, *2*, 669−677.
(4) Capaldi, R. A.; Aggeler, R. *Trends Biochem. Sci.* **2002**, *27*, 154−160.
(5) Duncan, T. M.; Bulygin, V. V.; Zhou, Y.; Hutcheon, M. L.; Cross, R. L. *Proc. Natl. Acad. Sci. U.S.A.* **1995**, *92*, 10964−10968.
(6) Aggeier, R.; Ogilvie, I.; Capaldi, R. A. *J. Biol. Chem.* **1997**, *272*, 19621−19624.
(7) Weber, J.; Senior, A. E. *Biochim. Biophys. Acta* **1997**, *1319*, 19−58.
(8) Abrahams, J. P.; Leslie, A. G. W.; Lutter, R.; Walker, J. E. *Nature* **1994**, *370*, 621−628.
(9) Menz, R. I.; Walker, J. E.; Leslie, A. G. W. *Cell* **2001**, *106*, 331−341.
(10) Noji, H.; Yasuda, R.; Yoshida, M.; Kinoshita, K. *Nature* **1997**, *386*, 299−302.
(11) Yasuda, R.; Noji, H.; Yoshida, M.; Kinoshita, K., Jr.; Itoh, H. *Nature* **2001**, *410*, 898−904.
(12) Yagi, H.; Tozawa, K.; Sekino, N.; Iwabuchi, T.; Yoshida, M.; Akutsu H. *Biophys. J.* **1999**, *77*, 2175−2183.
(13) Tozawa, K.; Yagi, H.; Hisamatsu, K.; Ozawa, K.; Yoshida, M.; Akutsu, H. *J. Biochem.* **2001**, *130*, 527−533.
(14) Yoshida, M.; Sone, N.; Hirata, H.; Kagawa, Y. *J. Biol. Chem.* **1975**, *250*, 7910−7916.
(15) Yamazaki, T.; Lee, W.; Arrowsmith, C. H.; Muhandriam, D. R.; Kay, L. E. *J. Am. Chem. Soc.* **1994**, *116*, 11655−11666.
(16) Gardner, K. H.; Kay, L. E. *Annu. Rev. Biophys. Biomol. Struct.* **1998**, *27*, 357−406.

10.1021/ja045279o CCC: $27.50

p53 (67 kDa, 279 residues)[18] and homooctameric construct of 7, 8-dihygroneopterin aldose (110 kDa, 121 residues),[19] and detailed analysis of the single chain protein of Malate Synthase G (81.4 kDa, 723 residues)[20−22] has been performed. Furthermore, cross-correlated relaxation-enhanced polarization transfer (CRINEPT)[23] increases the sensitivity of NMR. Using TROSY and CRINEPT, Wüthrich and his colleagues obtained ^{1}H-^{15}N correlation spectra of the 900 kDa GroEL−GroES complex.[24,25] Kay and his colleagues recorded the methyl signals of a 305 kDa 14-mer protein, Clap, by cross-correlated relaxation enhanced ^{1}H-^{13}C spectroscopy.[21]

The overlapping of signals may be overcome by increasing the dimensions of a NMR spectrum. This approach, however, is difficult when the number of atoms increases to a great extent. Another approach is to decrease the number of observable peaks. Techniques for such an approach are specific labeling and segmental isotope-labeling. Specific labeling is useful for obtaining local information, but not suitable for obtaining global information. On the other hand, segmental isotope-labeling is a powerful technique for getting global information. Segmental labeling has been carried out by either intein splicing reaction or chemical ligation.[26−29] However, there is no application to a really large molecule. We have applied segmental labeling by intein splicing reaction to the β subunit of F_OF_1-ATP synthase in this work, and have succeeded in obtaining the detailed information on the conformational change of the β subunit monomer.

Materials and Methods

Intein Reaction and Purification. An intein, PI-*Pfu*I, from *Pyrococcus furiosus* was used for segmental isotope-labeling.[30] The PI-*Pfu*I and β subunit genes were cut in the middle of the sequence, respectively. The N- and C-terminal fragments of the β subunit genes were ligated with those of the PI-*Pfu*I genes in such a way that the β subunit fragments formed exteins. The ligation was carried out by PCR. The genes encoding the N-terminal parts of the β subunit (4 types) and PI-*Pfu*I intein (1−160 residues) were amplified separately using PCR primers containing nucleotide sequences corresponding to a linker, Gly-Gly-Gly, and the overlapping sequences. The two PCR products were mixed and annealed. The ligated gene of the β subunit-intein precursor was obtained by PCR and then cloned into pET32a (Novagen) at the NdeI and BamHI restriction sites. The genes encoding the C-terminal parts of the PI-*Pfu*I intein (161−454 residues) and β subunit (4 types) were obtained similarly except that Thr-Gly was used as a linker. *E. coli* BL21 (λDE3) was transformed with each plasmid, and then grown at 37 °C in 1 L of LB medium or 80% D_2O M9 minimal medium containing 0.5 g $^{15}NH_4Cl$ and 2 g ^{13}C glucose as the sole nitrogen and carbon sources, respectively. Gene expression was induced with 1 mM IPTG (isopropyl-β-D-thiogalactopyranoside) at $OD_{600} = 0.5$, followed by incubation for 4 h. After cell disruption by sonication, the N-terminal fragments were dissolved in the supernatant, while the C-terminal fragments were precipitated as inclusion bodies. The C-terminal fragments were solubilized with buffer A (20 mM Tris/HCl, 1 mM EDTA, 1 mM DTT (dithiothreitol), pH 8.0) containing 6 M GdnHCl (guanidine hydrochloride). The N- and C-terminal precursors were mixed together in buffer A containing 6 M GdnHCl and 50% glycerol. The mixture was dialyzed against buffer A at 4 °C for 12 h to remove the denaturant. Then, the solution was heated to 70 °C for 1 h for splicing. The ligated β subunit was purified on an ion exchange column of Hitrap Q and a hydrophobic column of Hitrap Phenyl Sepharose with a NaCl gradient (0−500 mM) and an ammonium sulfate gradient (30−0 w/v saturation) in buffer A, respectively. Additional residues, Gly-Gly-Gly-Thr-Gly, were introduced at the ligation site.

NMR Measurements. For NMR measurements, the protein was dissolved at 0.2−0.4 mM in 20 mM Tris/HCl buffer (pH 8.0), containing 1 mM DTT, 1 mM NaN_3 and 10% D_2O. Sequential assignment was carried out for the four kinds of regionally U-[^{13}C,^{15}N,^{2}H] labeled β subunit. To check the assignments, amino acid specifically ^{15}N labeled β subunits were used. For the measurement of residual dipolar couplings (RDC), the β subunit monomer was partially aligned in a poly(ethylene glycol) (C12E5)/hexanol (molar ratio, 1/0.96) liquid crystal solution.[31] The weight ratio of β subunit to surfactant was 5%. For the nucleotide-bound β subunit, the molar ratio of MgADP to protein was five. The sample solution was completely homogeneous and pearly in color.

All NMR spectra were obtained with a Bruker DRX800 NMR spectrometer at 40 °C. The $^{15}N-^{1}H$ TROSY-HSQC spectra were recorded with a data size of 256 (^{15}N) × 1024 (^{1}H) complex points, and with spectral widths of 2912 Hz (F_1) and 9615 Hz (F_2). Backbone chemical shift assignments were carried out using the 3D TROSY-HNCO, 3D TROSY-HNCA, 3D TROSY-HN(CO)CA, 3D TROSY-HNCACB, 3D TROSY-HN(CO)CACB, and 3D ^{15}N-edited NOESY spectra with a matrix of 256 (^{15}N) × 1024 (^{1}H) × 1024 (^{1}H) points, and spectral widths of 2912 Hz (F_1), 9615 Hz (F_2), and 1111 Hz (F_3). The ^{1}H, ^{13}C, and ^{15}N carrier frequencies were set at 4.7, 54, and 118 ppm, respectively. ^{1}H-^{15}N dipolar couplings were recorded by means of a 2D IPAP-type ^{15}N-^{1}H HSQC correlation experiment.[32] All 2D IPAP experiments were carried out with 512 (^{15}N) × 1024 (^{1}H) complex points. The final data sets comprised 3072 (^{15}N) × 4096 (^{1}H) real points with digital resolutions of 0.84 (^{15}N) and 3.9 (^{1}H) Hz/point. All NMR data were processed using NMRPipe and NMRDraw,[33] and analyzed with Sparky.

Determination of the Alignment Tensor. The alignment tensors of weakly oriented samples were determined with program Module.[34] Residual dipolar coupling between spins i and j, D_{ij}, can be described in terms of the orientation (θ, φ) of the internuclear vector relative to a common alignment tensor for the molecule

$$D_{ij} = -\frac{S\gamma_i\gamma_j\mu_0 h}{16\pi^3 r_{ij}^3}\left\{A_a(3\cos^2\theta - 1) + \frac{3}{2}A_r\sin^2\theta\cos 2\varphi\right\} \quad (1)$$

where A_a and A_r are the axial and rhombic components of the alignment tensor, r_{ij} the internuclear distance, and S the order parameter. A_a, A_r, and the Euler angles (α, β, and γ) describing the orientation of the tensor relative to the PDB frame were obtained by least squares

(17) Pervushin, K.; Riek, R.; Wider, G.; Wüthrich, K. *Proc. Natl. Acad. Sci. U.S.A.* **1997**, *94*, 12366−12371.
(18) Mulder, F. A. A.; Ayed, A.; Yang, D.; Arrowsmit, C. H.; Kay, L. E. *J. Biomol. NMR* **2000**, *18*, 173−176.
(19) Salzmann, M.; Pervushin, K.; Wider, G.; Senn, H.; Wüthrich, K. *J. Am. Chem. Soc*. **2000**, *122*, 7543−7548.
(20) Tugarinov, V.; Muhandiram, R.; Ayed, A.; Kay, L. E. *J. Am. Chem. Soc.* **2002**, *124*, 10025−10035.
(21) Tugarinov, V.; Hwang, P. M.; Ollerenshaw, J. E.; Kay, L. E. *J. Am. Chem. Soc.* **2003**, *125*, 10420−10428.
(22) Tugarinov, V.; Kay, L. E. *J. Am. Chem. Soc.* **2003**, *125*, 13868−13878.
(23) Riek, R.; Wider, G.; Pervushin, K.; Wüthrich, K. *Proc. Natl. Acad. Sci. U.S.A.* **1999**, *96*, 4918−4923
(24) Fiaux, J.; Bertelsen, E. B.; Horwich, A. L.; Wüthrich, K. *Nature* **2002**, *418*, 207−211.
(25) Riek, R.; Fiaux, J.; Bertelsen, E. B.; Horwich, A. L.; Wüthrich, K. *J. Am. Chem. Soc*. **2002**, *124*, 12144−12153.
(26) Yamazaki, T.; Otomo, T.; Oda, N.; Kyogoku, Y.; Uegaki, K.; Ito, N.; Ishino, Y.; Nakamura, H. *J. Am. Chem. Soc*. **1998**, *120*, 5591−5592.
(27) Otomo, T.; Ito, N.; Kyogoku, Y.; Yamazaki, T. *Biochemistry* **1999**, *38*, 16040−16044.
(28) Xu, R.; Ayers, B.; Cowburn, D.; Muir, T. W. *Proc. Natl. Acad. Sci. U.S.A.* **1999**, *96*, 388−393.
(29) Romanelli, A.; Shekhtman, A.; Cowburn, D.; Muir, T. W. *Proc. Natl. Acad. Sci. U.S.A.* **2004**, *101*, 6397−6402.
(30) Ichiyanagi, K.; Ishino, Y.; Ariyoshi, M.; Komori, K.; Morikawa, K. *J. Mol. Biol.* **2000**, *300*, 889−901.
(31) Rückert, M.; Otting, G. *J. Am. Chem. Soc.* **2000**, *122*, 7793−7797.
(32) Ottiger, M.; Delaglio, F.; Bax, A. *J. Magn. Reson*. **1998**, *131*, 373−378.
(33) Delaglio, F.; Grzesiek, S.; Vuister, G. W.; Zhu, G.; Pfeifer, J.; Bax, A. *J. Biomol. NMR* **1995**, *6*, 277−293.
(34) Dosset, P.; Hus, J.-D.; Marion, D.; Blackledge, M. *J. Biomol. NMR* **2001**, *20*, 223−231.

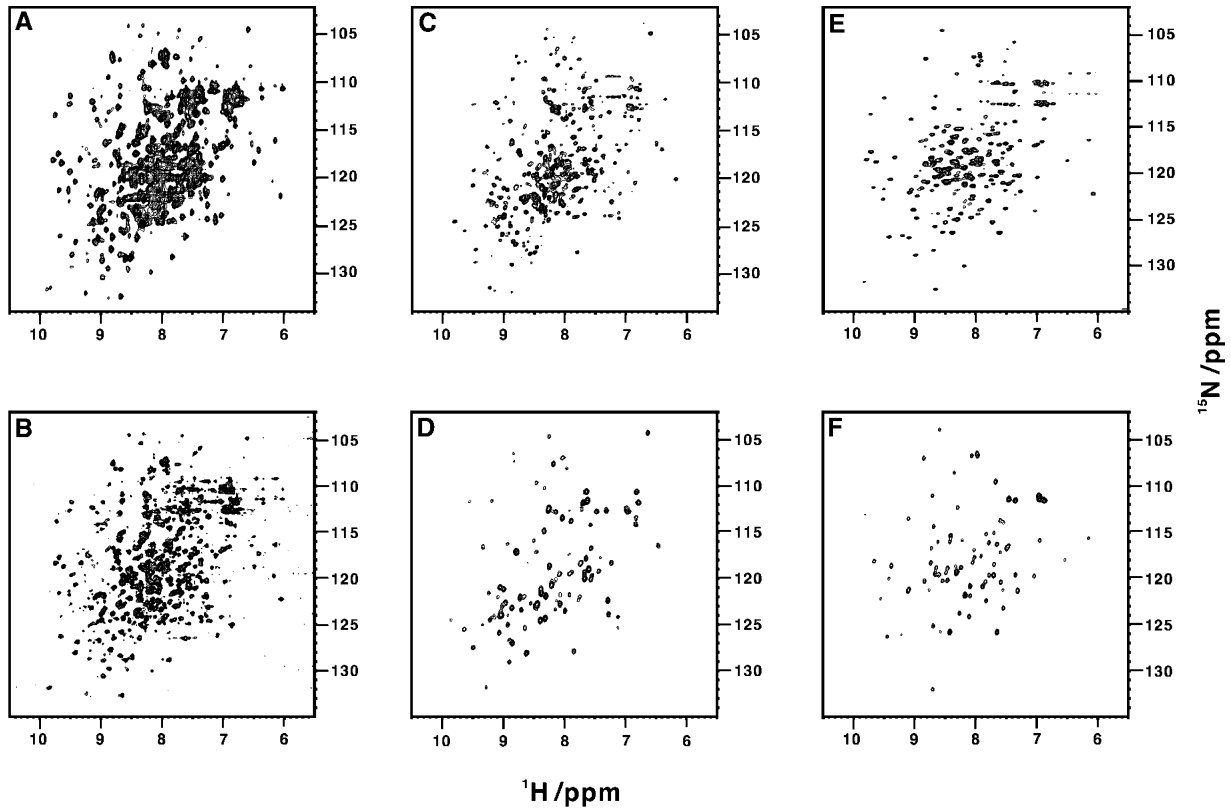

Figure 1. Two-dimensional ^{1}H−^{15}N HSQC (A) and TROSY-HSQC (B, C, D, E, and F) spectra (at 800 MHz for ^{1}H) of ^{15}N uniformly and regionally labeled β subunits. A and B; uniformly labeled β. C, D, E and F; β subunits ^{13}C, ^{15}N-labeled in the 1−271, 1−124, 272−473, and 391−473 segments, respectively.

minimization of the target function, χ^2, over all couplings associated with a given domain

$$\chi^2 = \sum_n (D_{ij}^{\exp} - D_{ij}^{calc})^2/{\sigma_{ij}}^2 \qquad (2)$$

where σ_{ij} is the uncertainty in the experimentally measured couplings. The standard coordinate file of the β subunit obtained from the crystal structure of the $\alpha_3\beta_3$ complex (PDB entry 1SKY) was converted to a new file that includes proton coordinates generated with Insight II. The experimental uncertainty, σ_{ij}, was estimated to be 0.5 Hz for all signals and the order parameter, S, was assumed to be one.

Results

Since β subunit of TF_1 consists of 473 amino acids,[14] a two-dimensional ^{1}H−^{15}N correlation NMR spectrum in the amide region showed poor resolution because of chemical shift overlapping and line broadening (Figure 1A). To suppress the line broadening, a TROSY-HSQC spectrum was obtained for the uniformly ^{15}N and ^{2}H labeled β subunit (Figure 1B). Although the quality of the spectrum was significantly improved, there is still severe signal overlapping. This problem was overcome by segmental isotope-labeling. We designed four kinds of β subunits, which are labeled in the segments comprising residues 1−271, 1−124, 272−473, and 391−473, respectively, with ^{15}N, ^{13}C, and ^{2}H. The other halves are not isotope-labeled. The cutting sites of the β subunit gene were set in loop regions with reference to the crystal structure of $TF_1\alpha_3\beta_3$.[35] ^{1}H−^{15}N TROSY-HSQC spectra of the four kinds of regionally isotope-labeled proteins were successfully obtained (Figure 1C,D,E, and F). The signal resolution was significantly improved in these spectra. The expected signal numbers are 259, 115, 191, and 80 for spectra C, D, E, and F, respectively, including the residues added through the intein reaction. All spectra completely coincide with the corresponding parts of the spectrum of the uniformly ^{15}N labeled authentic β subunit except for the signals of the inserted amino acid residues, confirming the intact structure of the ligated β subunit. Sequential assignment was carried out using 3D TROSY-HNCO, 3D TROSY-HNCA, 3D TROSY-HN(CO)CA, 3D TROSY-HNCACB, 3D TROSY-HN(CO)CACB, and 3D ^{15}N-edited NOESY spectra for the four kinds of ^{13}C/^{15}N/^{2}H labeled β.

The four kinds of spectra were assigned as follows. Because the region giving rise to the signals in spectrum C in Figure 1 contains the amino acid residues in spectrum D, spectrum D was assigned at first and then unassigned signals in spectrum C were assigned. The same procedure was carried out for spectra E and F. To confirm the sequential assignment, amino acid specific ^{15}N labeling was performed for Tyr, Thr, Lys, Ser, and Gly. Thus, 89% of the NH (402/451), 89% of the C_α (417/473), 83% of the C_β (357/431), and 90% of the CO (425/473) signals of the β subunit were assigned. The chemical shift values have been deposited in BioMagResBank (accession no. 5886).

The unassigned residues include the sequences 156−163, 188−201, 301−310, and 316−322 (colored white in Figure 2A). The signals of most unassigned residues (34 out of 49) are missing in the spectra. There could be two reasons for the missing. Since the spectra were measured at pH 8.0, the fast exchange of amide protons in the flexible regions would broaden

(35) Shirakihara, Y.; Leslie, A. G. W.; Abrahams, J. P.; Walker, J. E.; Ueda, T.; Sekimoto, Y.; Kambara, M.; Saika, K.; Kagawa, Y.; Yoshida, M. *Structure* **1997**, *5*, 825−836.

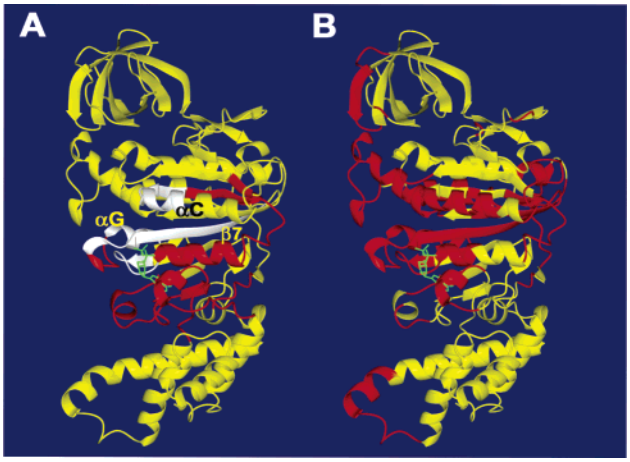

Figure 2. Comparison of the chemical shift perturbation in the monomer with the conformational change in F_1 for β subunit. (A) The chemical shift perturbation larger than 0.1 ppm for $\{(\Delta\nu_H)^2 + (0.15 \times \Delta\nu_N)^2\}^{1/2}$ on binding of MgADP to the β subunit is mapped on the closed form of the MF_1 β subunit.[8] The residues perturbed and unperturbed are colored red and yellow, respectively. White indicates the residues whose signals were not assigned. The ratio of MgADP to protein is 3. Helices, αC and αG, and a β sheet, β7, are indicated in the figure. The bound nucleotide is shown in green. (B) Local conformational change in the β subunit between the empty (open) and ADP-bound (closed) forms. It was evaluated by the distance of the same C_αs in different forms (d_{oc}) calculated for two cases. At first, N-halves of the two forms were superimposed with the smallest RMSD (used residues, 9−120 and 216−297). Then, C-halves were superimposed (330−415 and 420−474). Residue numbers are for MF_1. The region with a large difference is shown in red. Namely, $d_{oc} \geq 0.8$ Å for both cases. RMSD between the ADP and AMPPNP bound forms is about 0.8 Å. The surface on the left in this figure interacts with the γ subunit in F_1. These figures were drawn using Mol Mol.

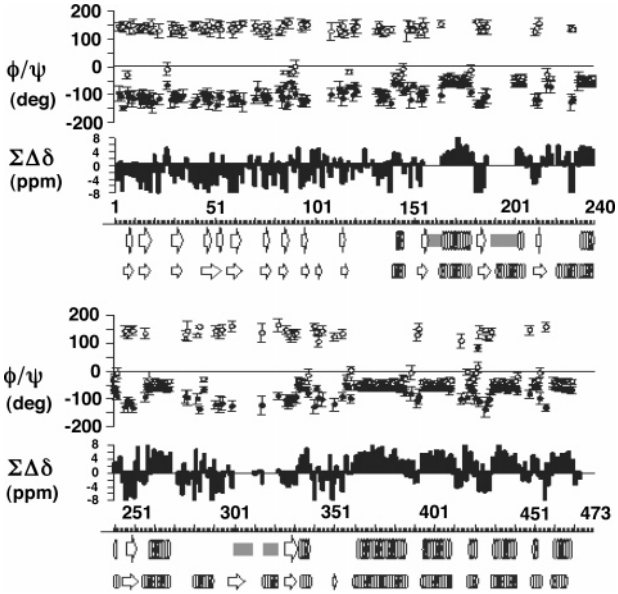

Figure 3. Chemical shift deviation (CSD) from a random coil and TALOS-derived ϕ/ψ angles with the β subunit sequence. The ϕ and ψ angles are presented as black and white circles with error bars, respectively, for residues where 9 or 10 matched in 10 database. CSD was obtained from the equation $\Sigma\Delta\delta = \Delta\delta C^\alpha - \Delta\delta C^\beta + \Delta\delta C'$. The chemical shifts of $^{13}C^\alpha$, $^{13}C^\beta$, and $^{13}C'$ in the random coil are subtracted from those obtained for the β subunit monomer. The secondary structure elements commonly predicted from the TALOS and CSD analyses are shown in the upper row at the bottom. Gray boxes indicate unassigned regions. The secondary structure elements in the lower row are those from the crystal structure of the $TF_1\alpha_3\beta_3$ complex (PDB code 1sky).[35]

or extinguish the signals. On the other hand, some aromatic rings of these residues showed doublets.[12,13] The exchange between these conformations could be the second reason of the signal broadening. Although the doublets became singlets on MgADP binding, the missing signals were not recovered. Therefore, the major reason of the loss of signals should be the fast exchange of amide protons in the flexible regions, which include α helices (αC and αG), a β sheet (β7), and the P-loop that form a conical tunnel.[8] This indicates that even an α helix is flexible in the isolated β subunit. This is consistent with the protease susceptibility of helix αC.[36]

To examine the conformational change induced by the nucleotide binding, the protein solution was titrated with MgADP. The signals of the 136−139, 164−186, 209−212, 311−314, 328−352, and 410−430 residues shifted in the presence of MgADP. These regions are mapped in red on the crystal structure of MgADP-bound β of MF_1 in Figure 2A. The 328−352 and 410−430 sequences form the binding pocket for the adenine ring of ADP in the crystal structure, suggesting that the chemical shift perturbations can be ascribed to direct interaction with adenine. In contrast, those in the other sequences can be ascribed to conformational changes induced by nucleotide binding. As can be seen in Figure 2A, these sequences fall in the hinge region and its proximity. This is in good agreement with previous results obtained on NMR analysis of Tyr and His residues, for which a conformational change from the open to the closed form was proposed.[12,13]

In the open and closed forms in the crystal structure of MF_1,[8] the relative orientations of the N- and C-terminal domains are different. Therefore, the domain orientation would provide direct information on the structures of the β subunit in different states. To obtain such information, two kinds of the β subunits labeled in the N-terminal (1−124) and C-terminal (390−473) domains, respectively, were used. Each one was partially aligned in liquid-crystal composed of poly(ethylene glycol) (C12E5)/hexanol (molar ratio, 1/0.96), and the residual dipolar couplings (RDC) were measured in the absence and presence of MgADP. RDCs were obtained for 65 and 40 residues for the 1−124 and 391−473 labeled β subunits, respectively.

Discussion

Chemical Shift Analysis of the β Subunit Monomer. The C_α, C_β, C′, and N chemical shifts of the assigned residues were analyzed with TALOS to estimate dihedral angles ϕ and ψ.[37] These angles could be predicted at high reliability (matching 9 or 10 in the 10 database) for 268 residues, corresponding to 67% of the 402 residues. The obtained angles are presented in Figure 3. The secondary structures were predicted on the basis of TALOS angles and the results of chemical shift deviation (CSD) analysis,[38] and are shown at the bottom of Figure 3. The N- and C-terminal domains of the $TF_1\beta$ monomer are composed of β-sheets and α-helices, respectively, in good agreement with the structures in the $TF_1\alpha_3\beta_3$ complex.[37] Comparison of the secondary structures of the monomer with those of $\alpha_3\beta_3$ strongly suggested that the general fold of the isolated β subunit is similar to that in $\alpha_3\beta_3$ despite the absence of helix 279−290. The crystal structure of the $TF_1\beta$ subunit in $\alpha_3\beta_3$ is in good agreement with the open form of the β subunit in the MF_1 crystal structure.

(36) Tozawa, K.; Odaka, M.; Date, T.; Yoshida, M. *J. Biol. Chem.* **1992**, *267*, 16484−16490.
(37) Cornilescu, G.; Delaglio, F.; Bax, A. *J. Biomol. NMR* **1999**, *13*, 289−302.
(38) Wishart, D. S.; Bigam, C. G.; Holm, A.; Hodges, R. S.; Sykes, B. D. *J. Biomol. NMR* **1995**, *5*, 67−81.

One of the major differences in the secondary structure between the open and closed forms of MF_1 is in residues N174−Y178 in the nucleotide-binding domain. This region takes on an α-helix conformation in the open form, but an extended conformation in the closed form. The secondary structure predicted for this region in the β subunit monomer with TALOS and CSD was an α-helix. So, the $TF_1\beta$ monomer should take on the open form in the absence of a nucleotide.

The chemical shift perturbations shown in Figure 2A are in good agreement with our earlier NMR results,[12,13] a conformational change from the open to the closed form taking place on nucleotide binding being proposed. In the MF_1 crystal structure, the conformational variations between the open and closed forms only occur in the hinge region and its proximity besides the adenine binding pocket and the regions interacting with the γ subunit. This is shown in Figure 2B. The perturbed regions in Figure 2A are quite similar to the regions with great conformational variations (colored red) in Figure 2B except for the regions interacting with the γ subunit. It should be indicated that most of the flexible regions colored white in Figure 2A are included in the red regions in Figure 2B. Thus, we can conclude that the conformational change of the β monomer induced by nucleotide binding is similar to that from the open to the closed form in the crystal structure of MF_1. From the perturbation map in Figure 2A, we can clearly identify the hinge as the stretch of N174−I182, where N174−Y178 takes on an α-helix conformation in the open form but an extended chain conformation in the closed form.

Relative Orientation of the N-Terminal and C-Terminal Domains. The effect of ligand binding on the backbone chemical shift showed that the nucleotide-binding domain of the β subunit monomer changes its conformation, responding to ligand binding. On the other hand, the intra-domain structures do not deviate for the N-terminal domain comprising residues 1−82 and the C-terminal domain comprising residues 372−473. Although chemical shift changes were observed for residues 410−420, this region includes Phe414 and Phe420 that interact with the adenine-ring, according to the crystal structure of the MF_1 $\alpha_3\beta_3\gamma$ complex.[8] Judging from the secondary structures in Figure 3, the main folds of two domains are similar for the monomer and the crystal structure of $\alpha_3\beta_3$. Therefore, we can use β subunits labeled at residues 1−124 (β(1−124)) and 390−473 (β(390−473)) to determine the relative orientation of the N- and C-terminal domains in the absence and presence of ligand. This will provide direct information on the conformational change suggested by the chemical perturbation shown in Figure 2A.

The experimentally measured $^1H-^{15}N$ RDCs of β(1−124) and β(390−473) were analyzed by a program Module, using the crystal structure of the corresponding region in the $\alpha_3\beta_3$ complex (1SKY) as the structure of the β monomer. At first, we used all of the observed RDCs for the analysis. However, the fitting was poor. This can be ascribed to the conformational difference between the β subunits in the monomer and $\alpha_3\beta_3$ complex. The influence of contacts with the neighboring α subunits is included for $\alpha_3\beta_3$. Furthermore, the loop and terminal regions would be flexible. Since the proton coordinates were generated by means of a software, the directions of some NH vectors could be different from the real ones. To avoid these problems, the residues located in either the α-helix or β-sheet were used for the calculation. The number of RDCs used were 43 and 20 for the N- and C-terminal domains, respectively. As a result, the fitting became much better, as can be seen in Figure 4. The alignment tensor and the Euler angles describing the orientation of the tensor relative to the PDB frame were obtained on the fitting. The Euler angles, and the axial and radial components, A_a and A_r, are summarized in Table 1 for each domain. The error ranges of the Euler angles were estimated by removing one point from the data set. The error range of Euler angle β was relatively small in comparison with that of α. All values were similar for the N-terminal domains of the ligand-bound and free β subunits. In contrast, the rhombicity and orientation of the tensor were different for their C-terminal domains. The relative orientations between the N- and C-terminal domains were determined using their alignment tensors, as shown in Figure 5. To evaluate the change in the relative orientation, the N-terminal domains of interest were completely superimposed. In the case of the ligand-free β subunit, the orientation of helix 399−409 in the C-terminal domain was different by 5° for the obtained and crystal (1SKY) structures (Figure 5B). In view of the error ranges shown in Table 1, these structures are practically the same. Since the crystal structure of the β subunit in the $\alpha_3\beta_3$ complex is in good agreement with the open form of the β subunit in the MF_1 $\alpha_3\beta_3\gamma$ crystal structure (1BMF), we can conclude that the β subunit monomer also takes on the open form in the absence of a nucleotide in solution.

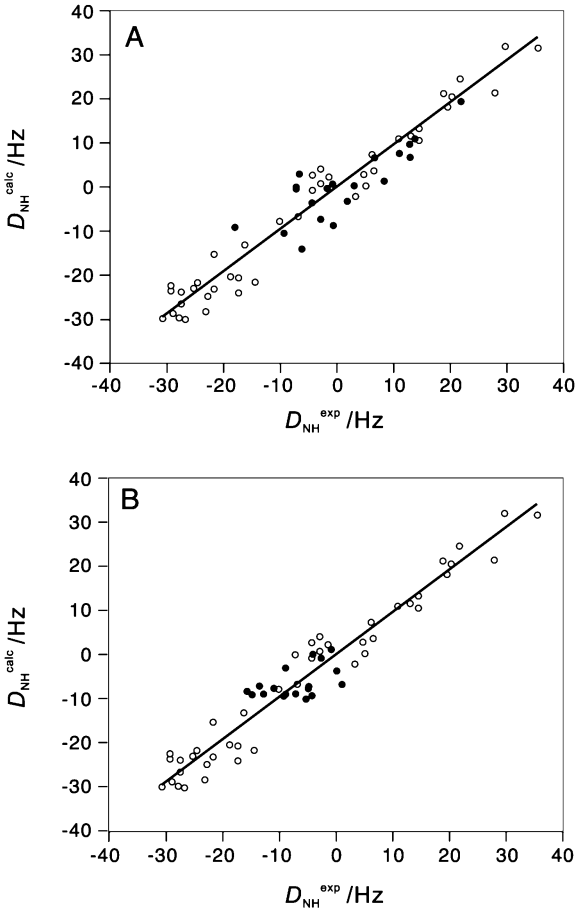

Figure 4. Comparison of the observed $^1H-^{15}N$ RDCs (D_{NH}^{exp}) with the values back-calculated using best-fit parameters and the crystal coordinates of the $\alpha_3\beta_3$ complex (D_{NH}^{calc}). A; In the absence of MgADP and B; in the presence of MgADP. The open and closed circles denote the data for the N- and C-terminal domains, respectively.

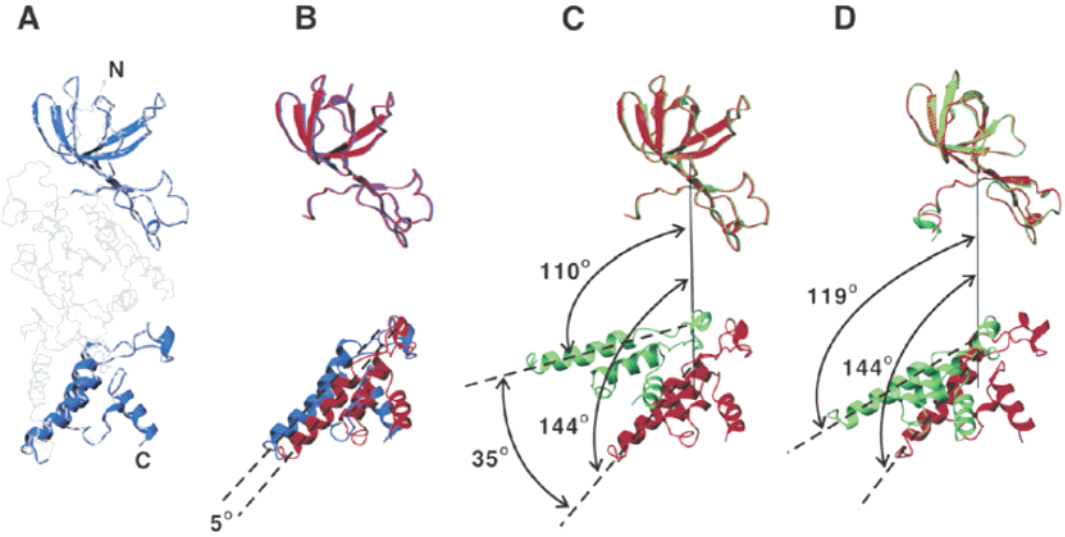

Figure 5. Relative orientations between the N- and C-terminal domains of the β subunit obtained from RDCs and crystal structures. A; The labeled segments (residues 1−124 and 391−473) are colored blue on the TF_1 β subunit.[35] B, C, and D; Comparison of the relative orientations with the N-domains of the two structures being superimposed. B; The relative orientation obtained from RDCs in the absence of MgADP (red), and that in the TF_1 $\alpha_3\beta_3$ crystal structure (blue). C; The orientations of the C-domain obtained from RDCs in the absence (red) and presence (green) of MgADP. The solid line is an axis connecting the centers of mass of the N- and C-domains of interest. Broken lines are the axes of helix 399−409. D; The orientations of the C-domain in the ligand-free (red) and MgADP-bound (green) forms of β subunit in the MF_1 $\alpha_3\beta_3\gamma$ crystal structure.[8] Solid and broken lines are the same as in C.

Table 1. Alignment Tensor **A**, Euler Angles and χ^2 for β Subunits Labeled in the N- or C-Terminal Domain in the Absence and Presence of MgADP[a,b]

	α (deg)	β (deg)	γ (deg)	$A_a \times 10^4$	$A_r \times 10^4$	χ^2
N(−MgADP)	−76.3 ± 3.4	115.7 ± 0.35	−45.2 ± 0.40	27.34	2.57	3.39×10^{-3}
N(+MgADP)	−75.3 ± 3.4	116.1 ± 0.40	−44.8 ± 0.42	26.24	2.55	3.20×10^{-3}
C(−MgADP)	−51.6 ± 6.2	113.6 ± 1.9	−56.4 ± 2.7	10.33	1.88	2.63×10^{-3}
C(+MgADP)	−49.2 ± 7.1	78.4 ± 3.5	−58.2 ± 3.2	9.32	0.65	1.91×10^{-3}

[a] The parameters describing the magnitude of tensor **A** and its orientation (Euler angles α, β, and γ) relative to the coordinate frame of the crystal structure (1SKY) were obtained with Module. [b] $\chi^2 = \sum_n (D_{ij}^{exp} - D_{ij}^{calc})^2/\sigma_{ij}^2$, where σ_{ij} is the uncertainty in the experimentally measured coupling.

To elucidate the conformational change of the β subunit monomer on MgADP binding, the relative orientation of the N- and C-terminal domains was examined. When the N-terminal domains of the ligand-bound and free structures obtained from RDCs were superimposed, the difference in Euler angle β of the C-terminal domain was 35°, as can be seen in Table 1. When an axis connecting the centers of mass of the N- and C-terminal domains is defined (solid straight lines in Figure 5C and D), the angles between this axis and the direction of helix 399−409 are 110° and 144° for the ligand-bound and free β subunits, respectively (Figure 5C). The difference in these angles (34°) is similar to that in Euler angle β. On the other hand, the difference of the corresponding angle between the open and closed forms in the MF_1 $\alpha_3\beta_3\gamma$ complex (1BMF) is 25° (Figure 5D). This finding indicates that the MgADP-bound structure is similar to the closed form in MF_1, taking the error range for the obtained angles in Table 1 into account. In view of the lack of a crystal structure of the β subunit monomer, a relatively large error range is inevitable. The rotation of the C-terminal domain around the same axis is small, as can be expected from Table 1, while it is about 10° in the MF_1 crystal structure. Because of the relatively large error range, it would be difficult to confirm this rotation at this stage. Nevertheless, it can be concluded on the basis of the clear change in Euler angle β that the binding of MgADP induced a conformational change from the open to the closed form in the β subunit monomer.

Concluding Remarks

The secondary structure based on the chemical shifts of the main chain atoms and the relative orientation of the N- and C-terminal domains determined by RDCs indicated that the β subunit monomer takes on the open form in the absence of a nucleotide. Chemical shift perturbation and the change in the relative orientation showed that the conformational change from the open to the closed form takes place in the β subunit monomer on MgADP binding. It should be noted that our earlier work showed that MgATP induces a similar conformational change.[12,13] This means that the conformational change from the open to the closed form on nucleotide binding is an intrinsic property of the β subunit. This intrinsic property should be one of the essential driving forces for the F_1 rotation. Actually, Wang and Oster proposed, on the basis of the results of thermodynamic analysis, that the elastic strain energy stored in the β subunit on nucleotide binding would cause the γ subunit to rotate.[39,40] Normal-mode analysis of structural plasticity also supported the idea of the storage of elastic energy in the β subunit.[41] Our results are consistent with this model. In contrast, our conclusion clearly contradicts the prediction of Böckmann and Grubmüller, on the basis of multinanosecond molecular dynamics simulation,

(39) Wang, H.; Oster, G. *Nature* **1997**, *396*, 279−282.
(40) Sun, S.; Chandler, D.; Dinner, A. R.; Oster, G. *Eur. Biophys. J.* **2003**, *32*, 676−683.
(41) Cui, Q.; Li, G.; Ma, J.; Karplus, M. *J. Mol. Biol.* **2004**, *340*, 345−372.
(42) Böckmann, R. A.; Grubmüller, H. *Nat. Struct. Biol.* **2002**, *9*, 198−202.
(43) Böckmann, R. A.; Grubmüller, H. *Biophys. J.* **2003**, *85*, 1482−1491.

that the conformation of the closed form is more stable than that of the open form for ligand-free β subunit.[42,43]

This work has shown that segmental isotope-labeling NMR is a really powerful method for investigating large proteins and supramolecular systems. In combination with improvement in pulse sequences, segmental isotope-labeling will open a new frontier for solution NMR.

Acknowledgment. This work was partly supported by Grant-in-Aids for Scientific Research from the Ministry of Education, Science, Technology, Sport and Culture of Japan (H.A.), and grants from JST (Core Research for Evolutional Science and Technology) (H.A.) and the Japan New Energy and Industrial Technology Development Organization (H.Y.).

JA045279O